

# Comparing Buffer Leakage in PolarMOSH on SiC and Free-Standing GaN Substrates

Mingda Zhu<sup>\*†</sup>, Bo Song<sup>\*†</sup>, Zongyang Hu<sup>\*†</sup>, Kazuki Nomoto<sup>\*†</sup>, Ming Pan<sup>‡</sup>, Xiang Gao<sup>‡</sup>,  
 Debdeep Jena<sup>\*†§</sup>, Huili Grace Xing<sup>\*†§</sup>

<sup>\*</sup> School of Electrical and Computer Engineering, Cornell University, Ithaca, NY, USA

<sup>†</sup> Department of Electrical Engineering, University of Notre Dame, Notre Dame, IN, USA

<sup>‡</sup> IQE RF LLC., Somerset, NJ, USA

<sup>§</sup> Department of Materials Science and Technology, Cornell University, Ithaca, NY, USA

Email: mz442@cornell.edu, grace.xing@cornell.edu

**Abstract**—GaN MOSHEMT or MOSFET on top of conducting (drift layer and drain electrode) layers is a building block for vertical GaN VDMOS power transistors. GaN MOSHEMTs incorporating a polarization-doped p-AlGa<sub>x</sub>N layer as the back barrier on top of conducting layers is named as PolarMOSH. In this work, we present a comparative study of PolarMOSH fabricated on SiC and free-standing GaN substrates. PolarMOSH wafers epitaxially grown on SiC substrates are found to suffer from large leakage currents, with or without Mg doping in the back barrier. Much lower leakage currents are achieved when PolarMOSH wafers are grown on free-standing GaN substrates. The large reduction of buffer leakage current is attributed to the much reduced dislocation density brought by free-standing GaN substrates. The PolarMOSH fabricated on free-standing GaN substrates has a current On/Off ratio  $> 10^{10}$  thanks to the low leakage current.

## I. INTRODUCTION

Free-standing GaN substrates with continuously improved quality and lowered cost have paved the way for realizing vertical GaN power devices, promising high conduction current but low on-resistance, high blocking voltage and fast switching speed. GaN Metal-Oxide-Semiconductor High Electron Mobility Transistor (MOSHEMT) or MOSFET on top of conducting (drift and drain electrode) layers is an essential element for vertical GaN VDMOS power transistors. GaN MOSHEMTs with a polarization-doped p-AlGa<sub>x</sub>N back barrier on top of conducting layers is named as PolarMOSH. It is a building block for the novel vertical GaN device PolarMOS [1], which takes advantage of the unique polarization properties of GaN for power applications. The cross section schematics of both PolarMOS and PolarMOSH are illustrated in Fig. 1.

Experimental realization of HEMTs with a p-type back barrier grown on unintentionally-doped (UID) GaN or n-GaN has been challenging due to the high buffer leakage as well as difficulty in junction placement due to Mg. In metal-organic chemical vapor deposition (MOCVD) growth, Mg tends to incorporate in subsequently grown layer [2], [3], resulting in compensation effects that prevent formation of two dimensional electron gas (2DEG). Chowdhury *et al.* [4] showed that the Mg diffusion could be suppressed through insertion of an AlN layer or a C doped GaN layer. However,

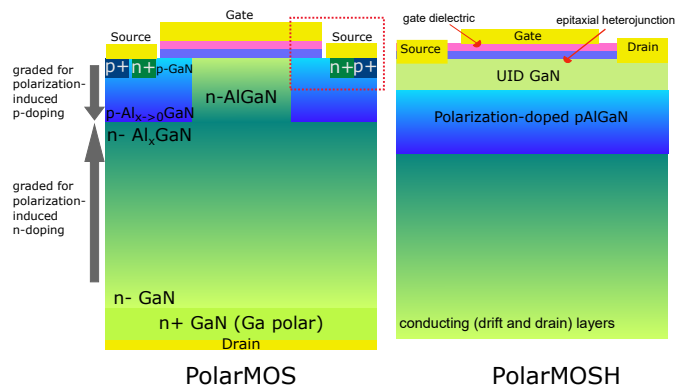


Fig. 1. Cross section schematics of PolarMOS (left) and PolarMOSH (right). PolarMOS is a novel vertical GaN power transistor [1]. PolarMOSH is a GaN MOSHEMT with a polarization-doped p-AlGa<sub>x</sub>N back barrier on top of conducting layers. It is a building block for PolarMOS, as illustrated by the red rectangle in the left figure.

in their experiments, Mg doping is carried out through ion implantation and the subsequent layers were regrown using molecular beam epitaxy. The regrowth interface often has high densities of impurities due to exposure to the atmosphere, which leads to high leakage current [5].

Here we present the first realization of PolarMOSHs, on free-standing GaN substrates and illustrate the adverse effect of dislocations on buffer leakage by comparing PolarMOSHs grown on SiC and GaN substrates. The experiments started with PolarMOSH epitaxial structures grown on SiC substrates, which show a persistently large buffer leakage current since the p-Al<sub>x</sub>Ga<sub>1-x</sub>N barrier does not effectively block leakage current between 2DEG channel and the underlying layers due to excessive amount of dislocations ( $\sim 10^9$  cm<sup>-2</sup>). The involvement of Mg doping is found to prevent the formation of 2DEG channel as well as alloyed ohmic contacts. Then the PolarMOSH epitaxial structure was carefully improved to reduce the effects of Mg doping on the 2DEG channel and grown on free-standing GaN substrates. The fabricated PolarMOSHs on free-standing GaN substrates show a high current On/Off ratio of  $> 10^{10}$  and a low drain leakage current

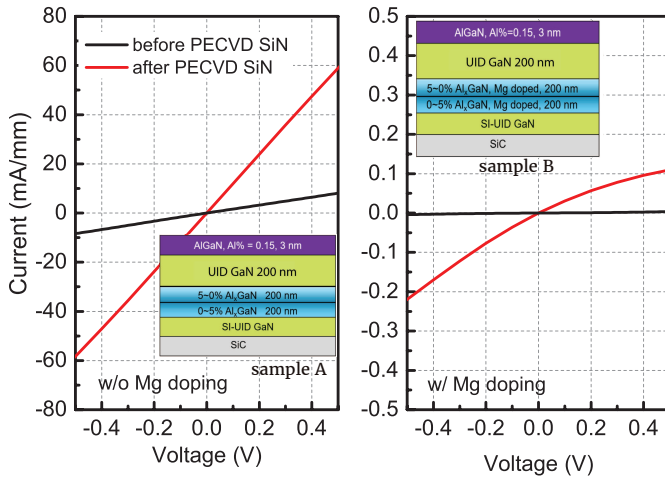


Fig. 2. Comparison of  $I$ - $V$  characteristics of a pair of ohmic contacts ( $2 \mu\text{m}$  separation) before and after  $20 \text{ nm}$  PECVD  $\text{SiN}_x$  deposition on (left) sample without Mg doping and (right) sample with Mg doping. Mg doping causes large decrease in measured currents.

of  $< 1 \text{ pA/mm}$ .

## II. EXPERIMENTS AND DISCUSSIONS

Two epitaxial structures were first designed to study the effects of graded  $\text{Al}_x\text{Ga}_{1-x}\text{N}$  and Mg doping. Both structures were grown on SiC substrates by MOCVD, consisting of a high-resistivity UID GaN layer,  $0\sim 5\%$  graded  $\text{Al}_x\text{Ga}_{1-x}\text{N}$ ,  $5\%\sim 0$  graded  $\text{Al}_x\text{Ga}_{1-x}\text{N}$  (with or without Mg),  $200 \text{ nm}$  UID-GaN,  $3 \text{ nm}$   $\text{Al}_{0.15}\text{Ga}_{0.85}\text{N}$ , while the only difference between the two device structures is the Mg doping in the back barrier. The epitaxial structures were designed for enhancement-mode (E-mode);  $20 \text{ nm}$  plasma-enhanced chemical vapor deposition (PECVD)  $\text{SiN}_x$ , which is found to increase the 2DEG concentration thus reduce sheet resistance [6], was deposited after Ohmic contacts formation (alloyed Ti/Al/Ni/Au). Figure 2 shows the comparison of  $I$ - $V$  characteristics of ohmic contacts before and after  $\text{SiN}_x$  deposition on both samples. As can be seen from both plots in Fig. 2,  $20 \text{ nm}$  PECVD  $\text{SiN}_x$  is effective in increasing measured current density for both epitaxial structures. However, the measured current density values are quite different. While the current through a pair of ohmic contacts separated by  $2 \mu\text{m}$  could reach  $60 \text{ mA/mm}$  at  $0.5 \text{ V}$  bias on the sample without Mg doping, it barely exceeds  $\sim 0.2 \text{ mA/mm}$  on the sample with Mg doping.

Fig. 3 shows the  $I$ - $V$  characteristics a pair of ohmic contacts separated by  $2 \mu\text{m}$  on the sample without Mg doping, showing a conduction current  $> 300 \text{ mA/mm}$  at  $5 \text{ V}$  bias. This  $I$ - $V$  behavior indicates that the channel 2DEG is compensated by Mg in the sample with Mg-doped back barriers, which is similar to Fe-doped or C-doped back barriers. Secondary ion mass spectrometry (SIMS) measurements (not shown here) show a residue Mg level of  $1 \times 10^{17} \text{ cm}^{-3}$  near the 2DEG channel region.

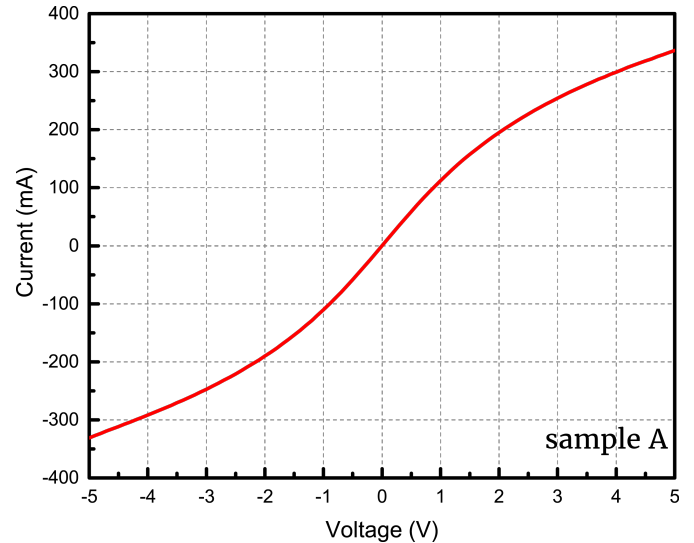


Fig. 3.  $I$ - $V$  characteristics of a pair of ohmic contacts ( $2 \mu\text{m}$  separation) after  $20 \text{ nm}$  PECVD  $\text{SiN}_x$  deposition on sample without Mg doping.  $I > 300 \text{ mA/mm}$  at  $5 \text{ V}$  bias.

Figure 4 shows the comparison of buffer leakage currents, with an excessive leakage current observed on both samples at  $20 \text{ V}$  bias. Device isolation on both samples are realized through  $100 \text{ nm}$   $\text{Cl}_2$  based dry etching using reactive ion etching (RIE). The buffer leakage test structure includes a pair of mesa isolated ohmic contacts separated by  $10 \mu\text{m}$ . Although the Mg doping reduces the buffer leakage current at low bias voltage range, the leakage currents are within the same order of magnitude at  $20 \text{ V}$ . The large dislocation density in GaN grown on SiC substrates have most likely resulted in the buffer leakage current increase as the bias voltage increases. To identify whether the leakage current flows through the buffer layer below the  $\text{Al}_x\text{Ga}_{1-x}\text{N}$  back barrier, additional etching of  $700 \text{ nm}$  on the PolarMOSH sample is carried out after PolarMOSH fabrication. The leakage current after  $100 \text{ nm}$  and  $800 \text{ nm}$  mesa etching is plotted in comparison in Fig. 5. Also plotted in Fig. 5 is the leakage current on a GaN-on-Si HEMT [7], [8]. A  $10^5\text{X}$  reduction in leakage current is observed when the etch depth is increased from  $100 \text{ nm}$  to  $800 \text{ nm}$ , suggesting that the  $\text{Al}_x\text{Ga}_{1-x}\text{N}$  layer and the UID GaN layer above contributes to most of the leakage current. However a further study is required to find out the exact amount of leakage current for each leakage path denoted in the upper inset plot in Fig. 5. The leakage current after  $800 \text{ nm}$  deep etching is still orders of magnitude larger than the GaN-on-Si HEMT, which has an impurity-doped semi-insulating GaN buffer layer. This indicates that the leakage path through the  $\text{Al}_x\text{Ga}_{1-x}\text{N}$  to the underlying SI-UID layer (as illustrated in the lower inset plot in Fig. 5), is due to the excessive amount of dislocations.

Following the mesa etch of  $100 \text{ nm}$  by RIE, the subsequent PolarMOSH fabrication process includes: gate lithography and RIE etching of PECVD  $\text{SiN}_x$ ,  $20 \text{ nm}$   $\text{Al}_2\text{O}_3$  deposition by atomic layer deposition (ALD) and gate metal deposition. The

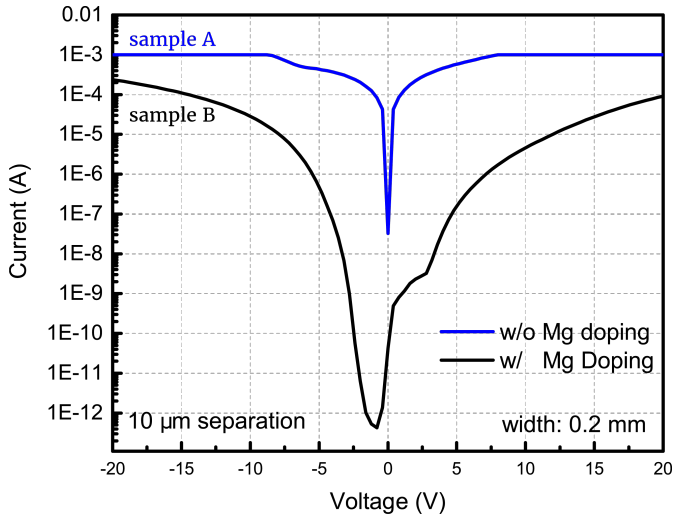


Fig. 4. Buffer leakage current comparison between sample A (without Mg doping) and sample B (with Mg doping). Although Mg doping reduces leakage current at low voltage bias, both samples show large leakage current at 20 V.

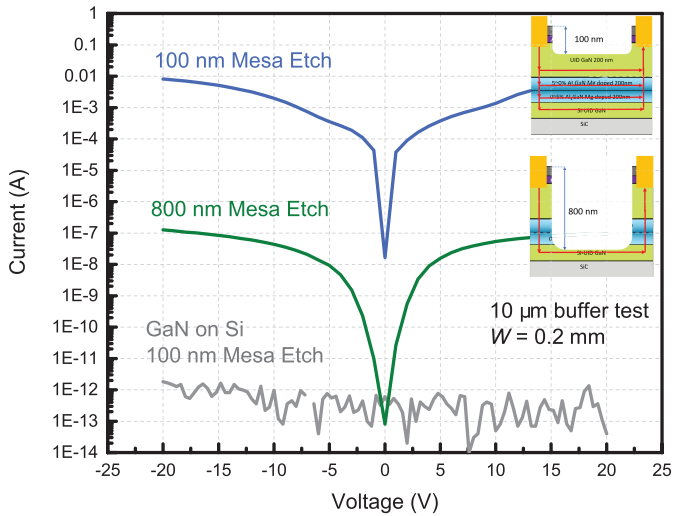


Fig. 5. Leakage current comparison between sample A with 100 nm and 800 nm mesa etching. Also plotted is the leakage current on a GaN-on-Si HEMT [7], [8]. A large leakage current reduction is observed after deep etching, although the reduced leakage current is still orders of magnitude larger than that on the GaN-on-Si sample. The possible leakage path after 100 and 800 nm etching are denoted as red arrow lines in the inset plots.

$I_D$ - $V_D$  characteristics of the PolarMOSH fabricated on the sample without Mg doping is shown in Fig. 6 along with its cross-section schematic. Although a clear gate modulation of drain current is seen from the plot, indicating the presence of electron channel, the excessive buffer leakage current prevents a complete turn-off of the drain current.

We have recently successfully demonstrated a series of GaN-on-GaN p-n diodes, which show unity ideality factor, avalanche breakdown and a record-setting figure-of-merit  $BV^2/R_{on}$  of  $> 16 \text{ GW/cm}^2$  [9]–[11]. This indicates that growing the PolarMOSH device structure on bulk GaN substrates (dislocation density  $\sim 10^6 \text{ cm}^{-2}$ ) is attractive in solving

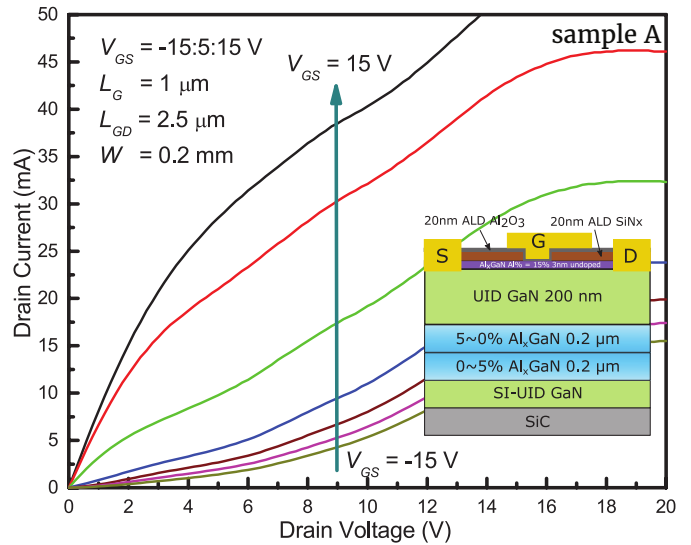


Fig. 6.  $I_D - V_D$  characteristics of MOSHEMT fabricated with sample A (No Mg doping). Clear gate modulation of drain current is shown. Large leakage current inhibits complete turn-off of drain current.

the buffer leakage issue. As illustrated in Fig. 7 (a), the epitaxial structure, starting from the GaN substrate, includes:  $7 \mu\text{m}$  Si doped n type GaN,  $1 \mu\text{m}$  graded  $\text{Al}_x\text{Ga}_{1-x}\text{N}$  with polarization induced doping,  $400 \text{ nm}$  Mg doped graded  $\text{Al}_x\text{Ga}_{1-x}\text{N}$ ,  $400 \text{ nm}$  UID GaN,  $20 \text{ nm}$   $\text{Al}_{0.15}\text{Ga}_{0.85}\text{N}$  and  $2 \text{ nm}$  GaN cap. This epitaxial structure is designed for depletion mode thus a quicker evaluation of the 2DEG channel is possible; the top AlGa<sub>x</sub>N barrier thickness can be reduced for E-mode devices. The PolarMOSH fabrication process is similar to that carried out on SiC substrate, except that the D-Mode epitaxy design eliminated the need of PECVD SiNx to form ohmic contacts. The fabrication process flow includes: ohmic contacts through Ti/Al/Ni/Au deposition and rapid thermal annealing, mesa isolation by dry etching,  $\text{Al}_2\text{O}_3$  deposition by ALD and gate metal deposition.

The  $I_D$ - $V_G$  characteristics of the fabricated PolarMOSH on free-standing GaN substrates is plotted in Fig. 7 (b), with the inset figure showing the cross section schematic. It is seen that an On/Off ratio  $> 10^{10}$  and a drain off-current  $< 1 \text{ pA/mm}$  are achieved. The large On/Off ratio, enabled by the low leakage current through the Mg doped graded  $\text{Al}_x\text{Ga}_{1-x}\text{N}$  layer as well as gate oxide, shows that the current blocking capability of Mg doped graded  $\text{Al}_x\text{Ga}_{1-x}\text{N}$  is vastly improved when grown on free-standing GaN substrates. This improvement in leakage current could be attributed to the much lower dislocation density in GaN grown on GaN substrates compared to GaN grown on SiC substrates [12],  $1 \times 10^6 \text{ cm}^{-2}$  versus  $1 \times 10^9 \text{ cm}^{-2}$ . As dislocations provide a vertical leakage path between the 2DEG above the p-layer and the conducting layer below the p-layer, reduction in dislocation density results in a reduction in measured buffer leakage current. The sharp turn-on behavior of drain current at  $V_G \sim 5 \text{ V}$  also shows that the compensation effects by Mg is limited.

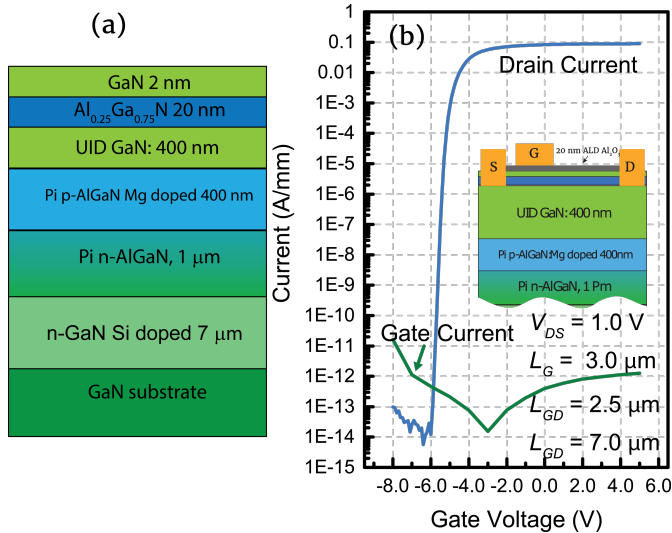


Fig. 7. (a) Epitaxial structure of PolarMOSH on free-standing GaN substrates. (b) The  $I_D - V_G$  characteristics of the fabricated PolarMOSH. The inset figure in (b) shows the cross section schematic of the fabricated PolarMOSH.

### III. CONCLUSION

In conclusion, we compare the leakage current behavior of PolarMOSH fabricated on SiC and free-standing GaN substrates. It is found out that the PolarMOSH fabricated on SiC substrates suffers from a large buffer leakage current. Though Mg doping in the graded  $\text{Al}_x\text{Ga}_{1-x}\text{N}$  back barrier reduces the leakage current, the channel residue Mg concentration is too high to form a 2DEG after depositing  $\text{SiN}_x$ . The PolarMOSH fabricated on free-standing GaN substrates, shows a low drain leakage current of  $< 1$  pA/mm and a high On/Off ratio of  $> 10^{10}$ . The much improved leakage characteristics could be attributed to the lower dislocation density of GaN grown on free-standing substrates than on SiC substrates. The device performance improvement shows the benefits of the superior quality of free-standing GaN substrates.

### REFERENCES

- [1] H. G. Xing, B. Song, M. Zhu, Z. Hu, M. Qi, K. Nomoto, and D. Jena, *Unique opportunity to harness polarization in GaN to override the conventional power electronics figure-of-merits*, in 2015 73rd Annual Device Research Conference (DRC), 2015, vol. 4395, no. 2001, pp. 5152
- [2] H. Xing, D. S. Green, H. Yu, T. Mates, P. Kozodoy, S. Keller, S. P. DenBaars, and U. K. Mishra, *Memory Effect and Redistribution of Mg into Sequentially Regrown GaN Layer by Metalorganic Chemical Vapor Deposition*, *Jpn. J. Appl. Phys.*, vol. 42, no. Part 1, No. 1, pp. 5053, Jan. 2003.
- [3] K. Tomita, K. Itoh, O. Ishiguro, T. Kachi, and N. Sawaki, *Reduction of Mg segregation in a metalorganic vapor phase epitaxial grown GaN layer by a low-temperature AlN interlayer*, *J. Appl. Phys.*, vol. 104, no. 1, p. 014906, 2008.
- [4] S. Chowdhury, B. L. Swenson, J. Lu, and U. K. Mishra, *Use of Subnanometer Thick AlN to Arrest Diffusion of Ion-Implanted Mg into Regrown AlGaIn/GaN Layers*, *Jpn. J. Appl. Phys.*, vol. 50, no. 10, p. 101002, Oct. 2011.
- [5] S. Chowdhury, M. H. Wong, B. L. Swenson, and U. K. Mishra, *CAVET on Bulk GaN Substrates Achieved With MBE-Regrown AlGaIn/GaN Layers to Suppress Dispersion*, *IEEE Electron Device Lett.*, vol. 33, no. 1, pp. 4143, Jan. 2012.

- [6] D. F. Brown, K. Shinohara, A. L. Corrion, R. Chu, A. Williams, J. C. Wong, I. Alvarado-Rodriguez, R. Grabar, M. Johnson, C. M. Butler, D. Santos, S. D. Burnham, J. F. Robinson, D. Zehnder, S. J. Kim, T. C. Oh, and M. Micovic, *High-Speed, Enhancement-Mode GaN Power Switch With Regrown n+ GaN Ohmic Contacts and Staircase Field Plates*, *IEEE Electron Device Lett.*, vol. 34, no. 9, pp. 11181120, Sep. 2013.
- [7] Bo Song, Mingda Zhu, Zongyang Hu, Meng Qi, K. Nomoto, Xiaodong Yan, Yu Cao, D. Jena, and H. G. Xing, *Ultralow-Leakage AlGaIn/GaN High Electron Mobility Transistors on Si With Non-Alloyed Regrown Ohmic Contacts*, *IEEE Electron Device Lett.*, vol. 37, no. 1, pp. 1619, Jan. 2016.
- [8] M. Zhu, B. Song, M. Qi, Z. Hu, K. Nomoto, X. Yan, Y. Cao, W. Johnson, E. Kohn, D. Jena, and H. G. Xing, *1.9-kV AlGaIn/GaN Lateral Schottky Barrier Diodes on Silicon*, *IEEE Electron Device Lett.*, vol. 36, no. 4, pp. 375377, 2015.
- [9] K. Nomoto, B. Song, Z. Hu, M. Zhu, M. Qi, N. Kaneda, T. Mishima, T. Nakamura, D. Jena, and H. G. Xing, *1.7-kV and 0.55 mΩ/cm<sup>2</sup> GaN p-n Diodes on Bulk GaN Substrates With Avalanche Capability*, *IEEE Electron Device Lett.*, vol. 37, no. 2, pp. 161164, Feb. 2016.
- [10] K. Nomoto, Z. Hu, B. Song, M. Zhu, M. Qi, R. Yan, V. Protasenko, E. Imhoff, J. Kuo, N. Kaneda, T. Mishima, T. Nakamura, D. Jena, and H. G. Xing, *GaN-on-GaN p-n power diodes with 3.48 kV and 0.95 mΩ/cm<sup>2</sup>: A record high figure-of-merit of 12.8 GW/cm<sup>2</sup>*, in 2015 IEEE International Electron Devices Meeting (IEDM), 2015, vol. 2016-Febru, pp. 9.7.19.7.4.
- [11] Z. Hu, K. Nomoto, B. Song, M. Zhu, M. Qi, M. Pan, X. Gao, V. Protasenko, D. Jena, and H. G. Xing, *Near unity ideality factor and Shockley-Read-Hall lifetime in GaN-on-GaN p-n diodes with avalanche breakdown*, *Appl. Phys. Lett.*, vol. 107, no. 24, 2015.
- [12] P. Kozodoy, J. P. Ibbetson, H. Marchand, P. T. Fini, S. Keller, J. S. Speck, S. P. Denbaars, and U. K. Mishra, *Electrical characterization of GaN p-n junctions with and without threading dislocations*, *Appl. Phys. Lett.*, vol. 73, no. 7, pp. 975977, 1998.